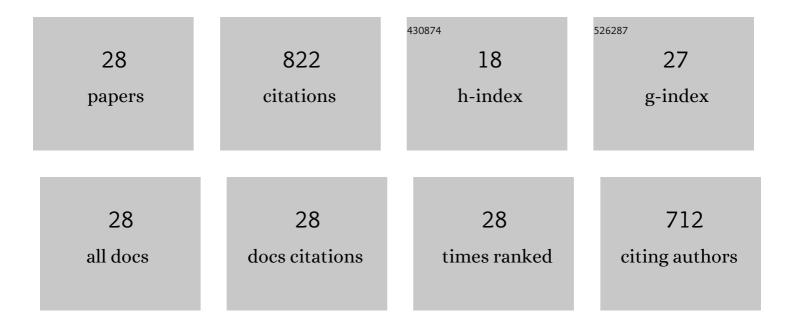


## List of Publications by Year in descending order

Source: https://exaly.com/author-pdf/6854879/publications.pdf Version: 2024-02-01



LIE HOU

#	Article	IF	CITATIONS
1	Pr <sub>2</sub> BaNiMnO <sub>7â^´Î´</sub> double-layered Ruddlesden–Popper perovskite oxides as efficient cathode electrocatalysts for low temperature proton conducting solid oxide fuel cells. Journal of Materials Chemistry A, 2020, 8, 7704-7712.	10.3	84
2	A new cobalt-free proton-blocking composite cathode La2NiO4+Î′–LaNi0.6Fe0.4O3â^'δfor BaZr0.1Ce0.7Y0.2O3â~δ-based solid oxide fuel cells. Journal of Power Sources, 2014, 264, 67-75.	7.8	78
3	High-aluminum fly ash recycling for fabrication of cost-effective ceramic membrane supports. Journal of Alloys and Compounds, 2016, 683, 474-480.	5.5	77
4	A high-performance cobalt-free Ruddlesden-Popper phase cathode La1·2SrO·8NiO·6FeO·4O4+l´ for low temperature proton-conducting solid oxide fuel cells. International Journal of Hydrogen Energy, 2019, 44, 7531-7537.	7.1	59
5	The effect of oxygen transfer mechanism on the cathode performance based on proton-conducting solid oxide fuel cells. Journal of Materials Chemistry A, 2015, 3, 2207-2215.	10.3	54
6	High performance ceria–bismuth bilayer electrolyte low temperature solid oxide fuel cells (LT-SOFCs) fabricated by combining co-pressing with drop-coating. Journal of Materials Chemistry A, 2015, 3, 10219-10224.	10.3	44
7	Cost-effective utilization of mineral-based raw materials for preparation of porous mullite ceramic membranes via in-situ reaction method. Applied Clay Science, 2016, 120, 135-141.	5.2	39
8	Ca-containing Ba0·95Ca0·05Co0·4Fe0·4Zr0·1Y0·1O3-Î′ cathode with high CO2-poisoning tolerance for proton-conducting solid oxide fuel cells. Journal of Power Sources, 2020, 453, 227909.	7.8	35
9	A novel in situ diffusion strategy to fabricate high performance cathodes for low temperature proton-conducting solid oxide fuel cells. Journal of Materials Chemistry A, 2018, 6, 10411-10420.	10.3	34
10	Effects of substrate orientation and solution movement in chemical bath deposition on Zn(O,S) buffer layer and Cu(In,Ga)Se2 thin film solar cells. Nano Energy, 2019, 58, 427-436.	16.0	33
11	High performance Ca-containing La2-xCaxNiO4+δ(0â‰ <b>¤</b> â‰ <b>9</b> .75) cathode for proton-conducting solid oxide fuel cells. International Journal of Hydrogen Energy, 2020, 45, 23422-23432.	7.1	32
12	Rational design of an in-situ co-assembly nanocomposite cathode La0.5Sr1.5MnO4+δ-La0.5Sr0.5MnO3-δ for lower-temperature proton-conducting solid oxide fuel cells. Journal of Power Sources, 2020, 466, 228240.	7.8	31
13	High-performance Ba(Zr 0.1 Ce 0.7 Y 0.2 )O 3â~δ asymmetrical ceramic membrane with external short circuit for hydrogen separation. Journal of Alloys and Compounds, 2016, 660, 231-234.	5.5	30
14	A novel composite cathode Er0.4Bi1.6O3–Pr0.5Ba0.5MnO3â~δ for ceria-bismuth bilayer electrolyte high performance low temperature solid oxide fuel cells. Journal of Power Sources, 2016, 301, 306-311.	7.8	30
15	A new cobalt-free composite cathode Pr 0.6 Sr 0.4 Cu 0.2 Fe 0.8 O 3â^'Î′ -Ce 0.8 Sm 0.2 O 2â^'Î′ for proton-conducting solid oxide fuel cells. Electrochimica Acta, 2015, 178, 60-64.	5.2	26
16	Cogeneration of ethylene and electricity in symmetrical protonic solid oxide fuel cells based on a La <sub>0.6</sub> Sr <sub>0.4</sub> Fe <sub>0.8</sub> Nb <sub>0.1</sub> Cu <sub>0.1</sub> O <sub>3â^î(electrode. Journal of Materials Chemistry A, 2020, 8, 25978-25985.</sub>	> 10.3	22
17	A strategy for improving the sinterability and electrochemical properties of ceria-based LT-SOFCs using bismuth oxide additive. International Journal of Hydrogen Energy, 2019, 44, 5447-5453.	7.1	20
18	Different ceria-based materials Gd0.1Ce0.9O2â^δ and Sm0.075Nd0.075Ce0.85O2â~δ for ceria–bismuth bilaye electrolyte high performance low temperature solid oxide fuel cells. Journal of Power Sources, 2015, 299, 32-39.	r 7.8	19

Jie Hou

#	Article	IF	CITATIONS
19	Fabrication of (Sm, Ce)O2â^´î´interlayer for yttria-stabilized zirconia-based intermediate temperature solid oxide fuel cells. Journal of Alloys and Compounds, 2015, 631, 255-260.	5.5	16
20	High performance BaCe0.5Fe0.5-xBixO3-l´ as cobalt-free cathode for proton-conducting solid oxide fuel cells. Journal of Alloys and Compounds, 2019, 790, 551-557.	5.5	15
21	One-step synthesis of CuCo2O4-Sm0.2Ce0.8O1.9 nanofibers as high performance composite cathodes of intermediate-temperature solid oxide fuel cells. International Journal of Hydrogen Energy, 2020, 45, 12577-12582.	7.1	11
22	A comparative study of the R-P phase Srn+1FenO3n+1 (n= 1, 2 and 3) cathodes for intermediate temperature solid oxide fuel cells. Ceramics International, 2020, 46, 19335-19342.	4.8	9
23	The effect of anode structure on the performance of NiO-BaZr0.1Ce0.7Y0.2O3-δ supported ceria-based solid oxide fuel cells. Ionics, 2019, 25, 3523-3529.	2.4	7
24	Advancing cathodic electrocatalysis <i>via</i> an <i>in situ</i> generated dense active interlayer based on CuO <sub>5</sub> pyramid-structured Sm <sub>2</sub> Ba <sub>1.33</sub> Ce <sub>0.67</sub> Cu <sub>3</sub> O <sub>9</sub> . Journal of Materials Chemistry A, 2022, 10, 15949-15959.	10.3	6
25	Rationally structuring proton-conducting solid oxide fuel cell anode with Ni metal catalyst and porous skeleton. Ceramics International, 2020, 46, 24038-24044.	4.8	5
26	A novel inhibiting water adsorption strategy to enhance the cathode electrocatalytic ability. Journal of Alloys and Compounds, 2021, 876, 160205.	5.5	3
27	The principles for rationally designing H-SOFC anode active layer. Materials Research Bulletin, 2022, 150, 111769.	5.2	3
28	Structural remodeling of Ni-based anodes for solid oxide fuel cells via static magnetic field. Scripta Materialia, 2020, 182, 86-89.	5.2	0